Published in final edited form as:
Neuroscience. 2013 October 10; 250: 263–274. doi:10.1016/j.neuroscience.2013.07.005.

Immunohistological demonstration of $Ca_V3.2$ T-type voltage-gated calcium channel expression in soma of dorsal root ganglion neurons and peripheral axons of rat and mouse

Kirstin E. Rose[1], **Nadia Lunardi**[1], **Annalisa Boscolo**[1], **Xinzhong Dong**[5], **Alev Erisir**[2,4], **Vesna Jevtovic-Todorovic**[1,3,4], and **Slobodan M. Todorovic**[1,3,4]

[1]Department of Anesthesiology, University of Virginia, Charlottesville, VA 22908

[2]Department of Psychology, University of Virginia, Charlottesville, VA 22908

[3]Department of Neuroscience, University of Virginia, Charlottesville, VA 22908

[4]Neuroscience Graduate Program, University of Virginia, Charlottesville, VA 22908

[5]Department of Neuroscience, Johns Hopkins University, Baltimore, MD 21205

Abstract

Previous behavioural studies have revealed that $Ca_V3.2$ T-type calcium channels support peripheral nociceptive transmission and electrophysiological studies have established the presence of T-currents in putative nociceptive sensory neurons of dorsal root ganglion (DRG). To date, however, the localization pattern of this key nociceptive channel in the soma and peripheral axons of these cells has not been demonstrated due to lack of isoform-selective anti-$Ca_V3.2$ antibodies. In the present study a new polyclonal $Ca_V3.2$ antibody is used to localize $Ca_V3.2$ expression in rodent DRG neurons using different staining techniques including confocal and electron microscopy. Confocal microscopy of both acutely dissociated cells and short-term cultures demonstrated strong immunofluorescence of anti-$Ca_V3.2$ antibody that was largely confined to smaller diameter DRG neurons where it co-localized with established immuno-markers of unmyelinated nociceptors, such as, CGRP, IB_4 and peripherin. In contrast, a smaller proportion of these $Ca_V3.2$-labeled DRG cells also co-expressed NF-200, a marker of myelinated sensory neurons. In the rat sciatic nerve preparation, confocal microscopy demonstrated anti-$Ca_V3.2$ immunofluorescence which was co-localized with both peripherin and NF-200. Further, electron microscopy revealed immuno-gold labelling of $Ca_V3.2$ preferentially in association with un-myelinated sensory fibres from mouse sciatic nerve. Finally, we demonstrated the expression of $Ca_V3.2$ channels in peripheral nerve endings of mouse hindpaw skin as shown by co-localisation with Mrgpd-GFP-positive fibres. The $Ca_V3.2$ expression within the soma and peripheral axons of nociceptive sensory neurons further demonstrates the importance of this channel in peripheral pain transmission.

Corresponding Author: Slobodan M. Todorovic, Department of Anesthesiology, University of Virginia Health System, Mail Box 800710, Charlottesville, VA 22908-0710, Phone 434-924-2283, Fax 434-982-0019, st9d@virginia.edu.

Authors declare no conflicts of interest.

Keywords

nociceptors; low-voltage-activated; T-currents; DRG; Ca^{2+}

1.1 Introduction

T-type calcium channels (T-channels) were originally discovered in the smaller dissociated neurons of dorsal root ganglia (DRG) (Carbone & Lux, 1984) where they regulate neuronal excitability by lowering thresholds for action potential initiation (Nelson *et al*., 2005; 2007). Furthermore, electrophysiological studies have suggested that T-channels are expressed in putative nociceptive DRG neurons. For example, acutely dissociated DRG cells expressing T-currents are typically of smaller and medium size diameter, the predominance of which are unmyelinated (C-type) and thinly myelinated (A-δ) sensory fibres (Scroggs & Fox, 1991; Schroeder *et al*, 1993; Cardenas *et al.,* 1995; Todorovic & Lingle 1998; Todorovic *et al*., 2001; Nelson *et al*., 2005; 2007; Coste *et al*., 2007). Further to these studies, we have previously used both acutely dissociated and intact DRG preparations to describe a novel DRG neuronal subtype, classed as T-rich cells. These T-rich cells have smaller diameters (26–31 μm), express high density T-currents, a robust response to capsaicin and antigenicity for isolectin B_4 (IB_4) (Nelson *et al*., 2005). Furthermore, T-rich DRG cells respond to high-threshold mechanical stimuli and co-express TTX-resistant sodium currents, further suggesting their nociceptive function (Coste *et al*., 2007). Recent studies have established that the $Ca_V3.2$ isoform of T- channels in DRG neurons plays a prominent role in supporting peripheral nociceptive transmission. This notion is based on the use of pharmacological agents that modulate these channels *in vitro* and also supporting *in vivo* studies where local injections of these agents into peripheral receptive fields of DRG neurons. For example, we reported that reducing agents, like L-cysteine, increase the amplitude of T-currents *in vitro* and following hindpaw injection *in vivo*, produced thermal and mechanical hyperalgesia of naive rats (Todorovic *et al*., 2001). Conversely, in the same study we showed that oxidizing agents, like DTNB, inhibit isolated T-currents *in vitro* and consequently induce analgesia when injected into rat hind paws *in vivo*. Importantly, we found that lipoic acid, another oxidizing agent, decreased DRG T-current amplitude *in vitro* and when locally injected into hind paws of wild-type (WT) mouse, induced analgesia. Further, the analgesic properties of lipoic acid were completely ineffective in $Ca_V3.2$ knock-out (KO) mice (Lee *et al*., 2009). In another study we found that several 5β-reduced neuroactive steroids, which robustly inhibit sensory neuron T-currents *in vitro*, produced peripheral analgesia *in viv*o (Todorovic *et al*., 2004). Similar methods were used by Barbara and colleagues (2009) who found that several analogues of lipoamino acids potently inhibited neuronal DRG T-currents *in vitro* and produced analgesia when locally injected into peripheral receptive fields of rat and WT mouse hindpaws. Further, this analgesic property was not seen in $Ca_V3.2$ KO mice. While these and similar studies strongly suggest that $Ca_V3.2$ T-channels are expressed within the peripheral nociceptive sensory neurons, a direct demonstration has been difficult due to paucity of selective anti-$Ca_V3.2$ antibodies. However, isoform-specific antibodies were used recently to study expression patterns of T-channels in the rat CNS (McKay et al., 2006). In this study we used a new commercially-available anti-$Ca_V3.2$ antibody to test the hypothesis that $Ca_V3.2$ channels are expressed in nociceptive subpopulations of acutely dissociated DRG neurons and in peripheral nociceptive fibres.

1.2 Experimental procedures

1.2.1 Cell culture

Three distinct variations of cultured human embryonic kidney (HEK) cells were used in the present study; standard non-transfected HEK cells, HEK cells with stable expression of

$Ca_V3.2$ (a gift from Dr. Paula Q. Barrett) and HEK cells transiently transfected with $Ca_V3.2$-EGFP (a gift from Dr. Jung-Ha Lee). Cells were maintained in DMEM (supplemented with 10% fetal bovine serum, penicillin G 100 mg/ml, streptomycin 100 μg/ml and L-glutamine 2 mM) and incubated in 5% CO_2 at 37°C. HEK cells with $Ca_V3.2$-GFP expression were incubated in standard media plus G418 to select for $Ca_V3.2$-GFP expressing cells. For transient transfection procedure, 0.5 μg of $Ca_V3.2$-GFP cDNA was transfected using lipofectamine 2000 (Invitrogen) standard protocol and cells were left for 24–48hr before being fixed for immunocytochemistry as we described previously (Orestes *et al.,* 2011).

1.2.2 Immunocytochemistry

T-channels are heteromeric protein complexes within the plasma membrane of many different cell types. Based on differences in molecular structure of α1 pore-forming subunits these channels are sub-dived as $Ca_V3.1$, $Ca_V3.2$ and $Ca_V3.3$. isoforms (reviewed in Perez-Reyes, 2003). Pore-forming α1 subunits are made of 4 transmembrane domains (D1–D4) interconnected with intracellular loops that vary in homology between T-channel isoform. Within this study we used anti-$Ca_V3.2$ rabbit polyclonal antibody raised against an epitope corresponding to amino acids 581–595 of rat intracellular loop connecting the D1 and D2 transmembrane domains of $Ca_V3.2$ (Sigma-Aldrich, catalogue number C1868). Western blot analysis of this antibody using ND7/23 cell line lysate has revealed band of appropriate molecular weight for $Ca_V3.2$ channel (Sigma technical information). Cells were detached and separated using 5% trypsin and then diluted using media prior to plating cells onto non-coated glass coverslips within 24 well plates. Cells were left on coverslips for 1–3 hours to allow attachment to glass and then wells were flooded with 4% PFA, 0.1M PB for 10min at 4°C. Cells were then rinsed with 0.01M PBS for 3 × 5 min at room temperature. Cells were then simultaneously permeabilised and non-specific binding was blocked using 0.1% Triton-X, 0.01M PBS supplemented with 5% donkey serum for 30 min at room temperature. Cells were rinsed with 0.01M PBS for 3 × 5 min at room temperature. Cells were then incubated in primary antibody at dilutions in 0.01M PBS stated below (Table 1).

Cells were then incubated with appropriate secondary antibody at dilution 1:2000 for 2 hr at room temperature (Table 1). Cells were then rinsed with PBS for 3 × 5 min at room temperature. Slides were then mounted using Vectashield plus DAPI (Vector Laboratories, Burlingame, CA) or VectaMount permanent mounting medium (Vector Laboratories). For each staining procedure the relevant solution without primary antibody was used as a negative control where cells were detected by the presence of DAPI staining contained within mounting media.

1.2.3 Animal experiments

All animal experiments were done in accordance with institutional and federal guidelines, including the National Institutes of Health *Guide for the Care and Use of Laboratory Animals* (NIH Publication No. 8023, revised 2002). All protocols used in this study have been approved by the University of Virginia Animal Care and Use Committee. Sprague-Dawley rats were obtained from Harlan Laboratories (Fredrick, MD), WT C57bl/6j mice and $Ca_V3.2$ KO mice were obtained from The Jackson Laboratory (Bar Harbor, ME). KO mice were repeatedly backcrossed for at least six generations against WT C57bl/6j mice.

1.2.4 Removal of tissue

Rats (7–14 day old) were killed by an overdose of anaesthesia (isoflurane) and rapidly decapitated. The rat was then placed on a dissection board with the dorsal surface facing uppermost. The skin overlying the lumbar region was cut away. A laminectomy of the lumbar region was then carried out. Specifically, the entire posterior backbone along with overlying ligaments and muscles was removed and was placed on a dissection board. The

excised section was pinned to the dissection board with the anterior surface facing uppermost. Scissors were used to make cuts through the lamina and body of the spinal vertebrae, starting at the anterior end, until the left and right sides of the column were separated. The spinal cord and meninges were then carefully removed using fine forceps to expose the DRG. Fine forceps were used to remove 6 – 8 lumbar DRG from both sides. The DRG were then placed into Tyrodes solution (in mM: 140 NaCl, 4 KCl, 2 $MgCl_2$, 2 $CaCl_2$, 0.5 $CdCl_2$, 10 glucose, and 10 HEPES, adjusted to pH 7.4) on ice. The attached dorsal roots and peripheral nerves were removed from the DRG using fine scissors. To remove a section of the sciatic nerve, the skin overlying the thigh was removed, and muscles overlying the nerve were separated using large scissors at mid-thigh level. If the sciatic nerve was attached to the muscle, a flat spatula was then used to carefully ease the nerve from the muscle and approximately 0.5 cm length of sciatic nerve was cut using fine sharp scissors at mid-thigh height.

1.2.5 DRG immunocytochemistry

We prepared acutely dissociated DRG neurons as previously described (Nelson *et al.*, 2005). DRG were plated onto non-coated glass coverslips and left for 1–3hr in incubator at 5% CO_2 at 37°C. Wells were then flooded with fixative and immunocytochemistry was carried out as for cultured cells. For immunohistochemistry of DRG sprouts, wells were flooded with standard media and left in incubator for up to 48 hours prior to fixation.

1.2.6 Nerve immunohistochemistry

The removed sciatic nerve was placed into 4% PFA, 0.1M PB, for 6 – 12 hr at 4°C. Sections were rinsed with 0.01M PBS for 3 × 5 min at room temperature. Fixed nerve was then cryoprotected in 30% sucrose in 0.01M PBS overnight at 4°C. Nerves were then embedded in OCT solution and longitudinal slices were cut on a cryostat at 30 μm and thaw-mounted onto poly-L-lysine coated slides. Immunohistochemistry was performed on free-floating slices. Slices were then simultaneously permeabilised and non-specific binding was blocked using 0.1% Triton-X, 0.01M PBS supplemented with 5% donkey serum for 1 hr at room temperature. Sections were rinsed with 0.01M PBS for 3 × 5 min at room temperature. Sections were then incubated in primary antibody at dilutions in 0.01M PBS stated in Table 1. Slices were then incubated with appropriate secondary antibody at dilution 1:2000 for 2 hr at room temperature (Table 1). Cells were then rinsed with 0.01M PBS for 3 × 5 min at room temperature.

1.2.7 Hind paw skin immunohistochemistry

Hind paw glaborous skin from WT and Mrgprd mice was removed using small fine scissors and placed in Zamboni's fixative (4% PFA, 15% picric acid, 0.1M PB) overnight at 4°C. Skin was then cryoprotected, embedded and sliced as nerve sections. Immunohistochemistry was performed on free-floating slices. Slices were simultaneously permeabilised and non-specific binding was blocked using 0.1% Triton-X, 0.01M PBS supplemented with 5% donkey serum for 1 hr at room temperature. Cells were rinsed with PBS for 3 × 5 min at room temperature. Slices were then incubated in primary and secondary antibody in 0.1% Triton-X, 0.01M PBS supplemented with 5% donkey serum at dilutions stated in Table 1.

1.2.8 Co-labeling studies

For all co-labeling studies, incubation with neurochemical marker preceded $Ca_V3.2$ labeling. Slides were then mounted using Vectashield plus DAPI (Vector Laboratories, Burlingame, CA). For each staining procedure the relevant solution without primary antibody was used as a negative control where cells were detected by the presence of DAPI staining contained within mounting media. All images were taken on a Zeiss LSM 510 Meta microscope, with

1 – 2 μm pinhole, detector gain and amplifier settings were adjusted at the beginning of the session and were not altered throughout each image capture session. Images were analysed using LSM image browser software (Version, 4,2,0,121, Zeiss). Cells where the nucleus was clearly identifiable were used in analysis of cell diameter. Cell diameter was gathered manually using LSM image browser measuring tool. Co-localization of cells positive for different cell markers was also carried out manually using LSM image browser. Percentages of positively marked cells are made with reference to the number of $Ca_v3.2$ positive cells which were also labeled with marker.

1.2.9 Electron microscopy (EM)-immunostaining

All steps were carried out at room temperature unless otherwise stated. Wild type (WT) mice (4 weeks old) were deeply anesthetised with isoflurane and transcardially perfused with 4% PFA, 1% GA in 0.1M PB. Sciatic nerve sections were then removed as described and placed in the same fixative for another 4 hr at 4°C. Nerve sections were then rinsed in 0.1M PB and then incubated in 1% osmium for 2 hr. Osmicated sections were rinsed with 0.1M PB for 3 × 3 min and then 50% ethanol for 3 min. Sections were then treated with 4% uranyl acetate for 1 hr. Sections were then dehydrated in sequential order in the following solutions; 70% ethanol for 1 min, 90% ethanol 5 min and then treated with 100% ethanol for 2 × 5 min. Sections were then dehydrated in acetone for 3 × 2 min, placed in 1:1 epon:acetone mixture for 2 hr and then in full epon overnight. Following this sections were then embedded in a flat-embedding mould and then cured for up to 72 hr in a 60°C oven. Capsules were then trimmed and ultrathin sections (85nm) were collected on 200 mesh copper grids using a Leica Ultracut UC7. Post-embedding immunostaining was then carried out. Grids were rinsed in 0.05M Tris buffer with 0.9% NaCl and TrirtonX-100 (TBST), pH 7.6 for 15 min. Grids were then incubated in $Ca_v3.2$ primary antibody (Sigma) at 1:50 in TBST, pH 7.6 for 2 hr. Grids were then rinsed in TBST, pH 7.4 for 2 × 5 min. Grids were then washed in TBST, pH 7.4 for 30 min and then conditioned in TBST, pH 8.2 for 5 min. Grids were then incubated in goat-anti-rabbit IgG conjugated gold (15nm) at 1:35 in TBST, pH 8.2 for 1 hr. Grids were washed in TBST, pH 7.4 for 2 × 5 min and H_2O for 2 × 5 min. Grids were then fixed in 2% gluteraldehyde for 10 min and then washed in H_20 2 × 5 min before being left to air dry.

In order to quantify the rate for association of gold particles with myelinated and unmyelinated axon membranes, 41 areas captured at 10,000X magnification, and contained both types of axons were examined, and the distance between each gold particle found in the pictures (n=2514) to its closest axon membrane was measured (Matsubara et al., 1996; Sun et al., 2007). To quantify clustering of gold particles with areas containing two different axon types, 10 pictures containing 467 gold particles were analysed.

Significance was determined using student t-test and χ-square test.

1.3 Results

1.3.1 $Ca_V3.2$ immunostaining was found within HEK 293 cells which stably or transiently express $Ca_v3.2$ channels

The specificity of the $Ca_V3.2$ antibody was tested using recombinant HEK cells overexpressing the human variant of the $Ca_V3.2$ T- channel isoform. Bright membranous $Ca_V3.2$ immunostaining was found within HEK cells which stably express the $Ca_V3.2$ channel (Figure 1A, C). In contrast, there was no detectable level of $Ca_V3.2$ immunolabelling in naïve HEK cells (Figure 1B). Similarly, HEK cells which had been transiently transfected with GFP-tagged $Ca_V3.2$, were also co-stained following $Ca_V3.2$ immunolabeling (Figure 1D).

1.3.2 $Ca_V3.2$ immunostaining was localised within smaller sensory neurons of heterologous rat DRG cultures

Previous *in vivo* studies using sharp electrodes have established that most small DRG neurons are nociceptive (Fang et al., 2006). Thus, we focused our study on acutely dissociated neurons with a somatic diameter <35 μm (Figure 2A). Indeed, we found that $Ca_V3.2$ immunostaining was found predominantly within smaller sensory neurons from rat DRG cultures with $Ca_V3.2$-positive neurons ranging from cell diameter of 9.7 μm to 32.1 μm (Figure 2D). The median cell diameter of $Ca_V3.2$ immunostained neurons was 19 ± 0.2 μm (n=557, Figure 2D). Interestingly, $Ca_v3.2$ immunolabeling was found throughout the cytoplasm of sensory neurons and in the somatic sprouts from cell soma (Figure 2B, 2C).

1.3.3 $Ca_V3.2$ immunostaining was found within the sensory neurons of WT mice but was not detected within $Ca_V3.2$-KO mouse DRG cultures

Similar to results from rat DRG preparations, $Ca_V3.2$ immunostaining was mainly present within smaller sensory neurons of dissociated DRG cultures from WT mice (Figure 3A). Importantly, only faint $Ca_V3.2$-positive immunostaining was detected in DRG cultures from $Ca_V3.2$-KO mice (Figure 3B). Similarly, we recently found that specific $Ca_V3.2$ staining was present only in spinal cord tissue from WT mice but not in spinal cord tissues from $Ca_V3.2$ KO mice (Jacus et al., 2012). Importantly, previous studies have shown that spinal cord tissues express mRNA for all three isoforms of Ca_V3 channels (Talley et al., 1999). This argues that anti-$Ca_V3.2$ antibody displays good selectivity.

1.3.4 $Ca_V3.2$-positive neurons were co-labelled with several different neuronal markers

Next we performed double-labelling studies with established sensory neuron markers. Figure 4 summarizes these data where $Ca_V3.2$ immunoflourescence is in red, marker in green, DAPI staining in blue and the overlay, where yellow represents co-labelling of marker and $Ca_V3.2$ (marked with arrows). Strikingly, we found that vast majority (94%) of $Ca_v3.2$ neurons were also labelled positive for peripherin, an established marker of small nociceptive unmyelinated sensory fibres, with the average cell diameter of these neurons was 16.7 ± 0.8 μm (Figure 4A). Overall, we found that 33 ± 4% of all peripherin-positive DRG cells also co-expressed $Ca_V3.2$ immunoreactivity.

Small unmyelinated DRG cells can be further divided on the basis of their peptide content into peptidergic CGRP-positive and non-peptidergic neurons expressing IB_4 antigen. We found that 11 ± 3% of all IB_4-positive neurons were co-labelled with anti-$Ca_V3.2$ antibody (Figure 4B). The average diameter of IB_4-$Ca_V3.2$-positive neurons was 20.0 ± 0.6 μm. Next we examined co-localisation of $Ca_V3.2$-expressing neurons and CGRP, a peptidergic nociceptor marker (Figure 4C). We found that 19 ± 3% of all CGRP-positive DRG neurons co-expressed $Ca_V3.2$ immunoreactivity. The mean cell diameter of $Ca_V3.2$-positive neurons, which also expressed CGRP, was 15.8 ± 0.5 μm. Finally, confocal microscopy revealed that a proportion (11 ± 3 %) of NF200-positve neurons, a marker of myelinated sensory fibres also co-localized with $Ca_V3.2$ immunoreactivity. The mean cell diameter of these $Ca_V3.2$ NF200 co-labelled cells was 22.7 ± 0.6 μm (Figure 4D).

1.3.5 Immunohistochemistry and EM-immunostaining revealed expression of $Ca_V3.2$-positive nerve fibres within rodent sciatic nerve

$Ca_V3.2$ immunostaining was found expressed within rat sciatic nerve sections (Figure 5). As expected from our preceding data, $Ca_V3.2$-positive fibres were also found to co-express peripherin (Figure 5A) and NF200 (Figure 5B) neurofilament markers. The left panels on Figure 5 show staining of the rat sciatic nerve with $Ca_V3.2$ antibody (red), the second panel shows staining of nerve with anti-peripherin (top) and anti-NF200 (bottom) antibodies

(green). The third panel shows DAPI staining of the sciatic nerve (blue), and right panels on Figure 5 shows overlay (yellow) as indicated by the arrows. Importantly, $Ca_V3.2$ immunofluorescence is similarly present in sciatic nerve sections from the WT mouse but is completely absent in the sciatic nerve tissue sections from the $Ca_V3.2$-KO mouse that was processed under identical conditions (data not shown).

To asses any presence of $Ca_V3.2$ channels in the distinct fibres from sciatic nerves of the WT mouse we next used EM. For these experiments we used gold-conjugated anti-$Ca_V3.2$ secondary antibodies. Figure 6 depicts a representative electron microphotograph from an 80 nm thin section of proximal sciatic nerve, showing a bundle of unmyelinated fibres (NONMYE) and partly showing 3 myelinated (MYE) fibres. Most gold-immunoparticles are confined to within the limits of neuronal membranes of NONMYE (arrows) while rare immunoparticles are observed close to axon membrane of the myelinated fibre, or over the myelin stacks (MYE). In control experiments, primary $Ca_V3.2$ antibody was omitted and only gold-conjugated secondary antibody was used. Under these conditions, no selective labelling was observed (data not shown). In order to confirm that gold labelling is selectively associated with axon membrane of unmyelinated fibres, we measured the distance of $Ca_V3.2$-bound immune-gold particles from axonal membranes of unmyelinated (NONMYE; Figure 7A, open bars on left panel) and myelinated (MYE; Figure 7A, cross hatched bars on right panel) sciatic nerve fibres of WT mouse. Counts of immunoparticles are grouped in bins of 0.05 μm ranging from 0 to 0.8 μm (Figure 7A). These data were used to construct curves of cumulative frequency of counts and to compare two functionally different classes of peripheral fibres (Figure 7B). Out of all gold particles, the closest membrane for which was an unmyelinated axon, 80% were within a 100 nm distance from the axon membrane. In contrast, when a myelinated axon membrane is the closest membrane for a gold particle, the distance between them was less than 100 nm at only 37% probability. About twofold ($p<0.001$ χ-square test) more particles were associated with NONMYE (80%) than MYE (37%) axonal membranes as determined by the distance of less than 100 nm (solid gray vertical line on Fig. 7B). Furthermore, gold particles were clustered more densely over fascicles containing unmyelinated axons: the density of gold dots over unmyelinated areas (3.1 ± 0.3 counts/μm^2) was significantly higher than the mean density (1.6 ± 0.1 counts/μm^2; $p<0.001$, n=10 pictures). In the same images the density in the myelinated areas (2.3 ± 0.4 counts/μm^2) vs. mean density was not significantly different ($p>0.05$, t-test, data not shown). Overall, our data with EM of peripheral nerves confirm our findings from acutely dissociated DRG cells that Cav3.2 is preferentially expressed in small unmyelinated sensory neurons.

1.3.6 Expression of $Ca_V3.2$-positive nerve fibres within peripheral skin nerve endings of the mouse

Finally, we performed experiments to study whether $Ca_V3.2$ channels are present in more distal peripheral axons located in the glabourous skin of mouse. For these experiments, immunohistochemistry of free-floating 25 μm thick skin sections was carried out followed by confocal microscopy. To facilitate our efforts in identifying functional nociceptive nerve endings, we took advantage of Mrgprd-GFP knock-in (KI) mouse. It has been established that this mouse is an excellent tool to visualize a subset of IB_4-positive polymodal nociceptors within skin (Zylka *et al.*, 2005; Liu *et al.*, 2009). Since we found that at least some IB_4-positive DRG cells are expressing $Ca_V3.2$ immunofluorescence (Figure 4B), we hypothesized that $Ca_V3.2$ channels in peripheral nociceptors may also co-localize with Mrgprd. Figure 7C summarizes our novel findings. Note that $Ca_V3.2$ immunoreactivity (Figure 8A, red colour) largely corresponds to Mrgprd immunoreactivity (Figure 8B, green colour) in the same section. This is confirmed by areas of yellow co-labelling on the merged fields (Figure 8D). Blue staining (Figures 8 C,D) represents DAPI staining of keratinocyte

cell nuclei and the border between dermis (less dense cells) and epidermis (very dense cells) is approximated by a white line on Figure 8C. This indicates that the above mentioned $Ca_V3.2$ and Mrgprd-positive nociceptive fibres are largely co-located along the inner side of the epidermis (arrowheads on Fig. 8D) and much less in epidermis (arrows on Fig. 8D). Overall our experiments demonstrate, for the first time, that $Ca_V3.2$ channels are expressed within nociceptive nerve endings and peripheral nerves.

1.4 Discussion

The DRG contains the cell bodies of primary sensory neurons which terminate within the periphery and whose central processes synapse and release neurotransmitters (e.g. neuropeptides and excitatory amino acids) in the spinal cord. Smaller diameter DRG neurons predominantly have slow-conducting unmyelinated C-fibres, while larger diameter neurons have faster A-type myelinated fibres (Harper & Lowson, 1985). There are several different types of cutaneous sensory receptors, which are characterized by fibre type and activating stimuli. Low threshold mechanoreceptors have large myelinated fibres (A-α and A-β) which transmit sensations of light touch, proprioception and vibration. High threshold mechanoreceptors have thinly myelinated axons (A-δ) and respond only to painful intense mechanical stimuli, while a subgroup of A-δ fibres responds to light touch (D-hair mechanoreceptor). C-polymodal nociceptors have unmyelinated (C) fibres and respond to intense harmful mechanical or thermal stimuli and to a variety of chemical irritants. There are both C and A fibres that respond to noxious mechanical and noxious heat stimuli. In this study, for the first time, we have demonstrated the expression pattern of $Ca_V3.2$ channels in different sub-populations of primary sensory neurons. The vast majority of $Ca_V3.2$-labeled DRG neurons in our preparation were co-stained with peripherin, an established marker of small diameter unmyelinated, C-type sensory neurons. The prominent co-expression of peripherin, as well as, the smaller cell diameter of $Ca_V3.2$-positive DRG neurons (median diameter of ~17 μm), strongly suggests that the majority of DRG neurons in our preparations expressing $Ca_V3.2$ protein are nociceptive. In contrast, we found that a smaller proportion of DRG cells in our preparation were co-labelled with $Ca_V3.2$ and NF-200, a marker of myelinated sensory fibres. These DRG cells also had somewhat larger cell diameters (median of ~23 μm), in comparison to those co-labelled with peripherin. Based on their small size, we propose that these NF-200 and $Ca_V3.2$-positive sensory neurons are most likely thinly myelinated, A-δ neurons, the predominance of which is also nociceptive.

Furthermore, we used other cell-specific markers to further characterize putative nociceptive DRG neurons. It is known that C fibre nociceptors can be subdivided on the basis of histological markers (Snider & McMahon, 1998; Stucky & Lewin, 1999; Hunt & Mantyh, 2001). One major group expresses pro-inflammatory peptides such as substance P and calcitonin-gene-related peptide (CGRP), and project to the most superficial layers of the spinal cord dorsal horn (e.g. lamina I and the outer zone of lamina II). A second group does not express substance P or CGRP, but can be identified by the presence of specific enzymes (e.g. fluoride-resistant acid phosphatase) or binding sites for the isolectin B_4 (IB_4). These non-peptidergic C-type fibres project to the slightly deeper inner lamina II of the spinal cord dorsal horn. Interestingly, histological differences may suggest distinct functional roles for nociceptors. While both classes of nociceptors are believed to respond to noxious chemical, thermal and mechanical stimuli, recent studies suggest that these two nociceptor cell types may contribute differentially to the generation and maintenance of pain. For example, peptidergic neurons appear to be the major effectors of neurogenic inflammation, releasing proinflammatory peptides such as substance P and CGRP from their peripheral terminals in response to activation. On the contrary, genetic studies strongly suggest that IB_4-positive, non-peptidergic nociceptors are more involved in chronic pain resulting from nerve injury (reviewed by Snider & McMahon, 1998). Our data reveals that some $Ca_V3.2$-positive DRG

cells are also positive for IB_4 and CGRP (Figure 4). In addition, we recently reported that DRG neurons which terminate within the superficial laminae of the spinal dorsal horn co-express $Ca_V3.2$ with IB_4 and CGRP markers (Jacus *et al.*, 2012). This would imply that $Ca_V3.2$ T-channels may be involved in both chronic neuropathic and inflammatory pain processing. Indeed recent functional studies support this notion. For example, $Ca_V3.2$ channels play an important role in neuropathic pain associated with animal models of peripheral diabetic neuropathy (Jagodic *et al.*, 2007; Latham *et al.*, 2009; Messinger *et al.*, 2009) as well as neuropathy resulting from chronic constrictive injury (CCI) to the rat sciatic nerve (Dogrul *et al.*, 2003; Bourinet *et al.*, 2005; Jagodic *et al.*, 2008; Takahashi *et al.*, 2010). There is also reasonably good evidence that $Ca_V3.2$ channels are involved in inflammatory pain responses as well since mice lacking $Ca_V3.2$ channels have reduced responses in the formalin test (Choi *et al.*, 2007) and antisense knock-down of $Ca_V3.2$ in DRG cells ameliorates pain in a rat model of irritable bowel disease (Marger *et al.*, 2011). Towards this end, we have recently found that during *in vivo* studies that a novel, selective and potent T-type channel blocker, TTA-P2, potently reduces inflammatory pain in the formalin test, as well as in a model of painful diabetic neuropathy (Choe *et al.*, 2011).

Confocal microscopy in our experiments revealed that $Ca_V3.2$ immunostaining was present uniformly throughout the cytoplasm of DRG cells. This particular subcellular staining pattern has been reported for other ion channels in DRG cells including $K_V1.4$ (Rasband *et al.*, 2001), $Na_V1.8$ and $Na_V1.9$ (Benn *et al.*, 2001), and also TRPV1 (Guo *et al.*, 1999). Cytoplasmic distribution of the $Ca_V3.2$ subunit may be a result of the intracellular organization of smaller sensory neurons, which have more compact and evenly distributed rough ER, with less filamentous structures (Lawson, 1979). The cytoplasmic distribution may also represent recently synthesized $Ca_V3.2$ protein in the endomembrane system, which appears uniformly throughout the cytoplasm (Rasband *et al.*, 2001)

Previous electrophysiological studies have also reported large $Ca_V3.2$-type currents in a subpopulation of cultured DRG cells with an average cell diameter 32–45 μm that represent putative non-nociceptive D-hair mechanosensory cells (Shin *et al.*, 2003; Dubreuil *et al.*, 2004; Coste *et al.*, 2007). It is unlikely that in our DRG preparation many of the cells could be putative D-hair mechanoreceptors since we focused mostly on smaller size DRG neurons (Figure 4D). Further, in our previous study, we showed that most acutely dissociated DRG cells expressing prominent T-currents and with somatic diameters from 30–40 μm were IB_4-positive, suggesting their nociceptive function (Jagodic *et al.*, 2007). Furthermore, we are not aware of any *in vivo* study that could substantiate the role of $Ca_V3.2$ channels in non-nociceptive mechanosensation.

Our data introduce much needed information regarding the expression of $Ca_V3.2$ channels in peripheral axons of the sciatic nerve and peripheral nerve endings in glaborous skin. This is important since many behavioural pain studies have indicated that $Ca_V3.2$ channels are expressed in the peripheral nerve terminals where they modulate the activity of cutaneous nociceptors. However, complimentary morphological evidence for such *in vivo* findings was lacking. Here we clearly demonstrate the presence of $Ca_V3.2$ immunoreactivity in unmyelinated and thus likely nociceptive peripheral axons of sciatic nerve and Mrgprd-positive nociceptor endings within glaborous skin. It is well established that somatic $Ca_V3.2$ currents are key regulators of subthreshold excitability within C-type sensory neurons (Nelson *et al.*, 2005; 2007). It remains to be determined whether $Ca_V3.2$ currents within the peripheral nociceptive axons and terminals of sensory neurons also play an important role in regulating membrane excitability. Towards this end, predominant localisation of $Ca_V3.2$ immuoreactivity in the dermal-epidermal border (Figure 8) suggests the possible role of $Ca_V3.2$ channels in the initiation of action potentials in the nociceptive nerves. Furthermore, it is also possible that T-channels expressed within the peripheral terminals of sensory

neurons may regulate secretion of neurotransmitters as suggested by a provocative study by Spitzer and colleagues (2008).

1.4.1 Conclusion

In conclusion, our data provide the first immunohistological demonstration of $Ca_V3.2$ channel expression in the soma and peripheral axons of nociceptive DRG neurons. Further functional studies are needed to investigate the function of these channels and their plasticity in physiological and pathological conditions such as chronic inflammatory and neuropathic pain disorders.

Acknowledgments

Our research is supported by NIH grant 3R01GM075229-04S109, American Diabetes Association 7-09-BS-190 (to S.M.T.), Dr. Harold Carron Endowment (V.J.-T) and NS054791 and GM087369 (to X.D.).

We would like to thank Dr. Paula Q. Barrett for kindly providing $Ca_V3.2$ stably transfected recombinant cells and Dr. Jung-Ha Lee for providing $Ca_V3.2$-EGFP plasmid for transient transfections of recombinant cells.

Abbreviations

DRG	dorsal root ganglion
T-channels	T-type calcium channels
Mrgprd	Mas-related G protein-coupled receptor D
NF 200	neurofilament 200
CGRP	calcitonin-gene-related-peptide
CNS	central nervouos system
IB_4	isolectin B4
GFP	green fluorescent protein
DTNB	di-thio nitro benzene
KO	knock-out
KI	knock-in
HEK	human embryonic kidney
EM	electron microscopy
ER	endoplasmic reticulum
MYE	myelinated
NONMYE	unmyelinated
WT	wild type

1.6 References

Barbara G, Alloui A, Nargeot J, Lory P, Eschalier A, Bourinet E, Chemin J. T-type calcium channel inhibition underlies the analgesic effects of the endogenous lipoamino acids. J Neurosci. 2009; 29(42):13106–14. [PubMed: 19846698]

Benn SC, Costigan M, Tate S, Fitzgerald M, Woolf CJ. Developmental expression of the TTX-resistant voltage-gated sodium channels Nav1.8 (SNS) and Nav1.9 (SNS2) in primary sensory neurons. J Neurosci. 2001; 21(16):6077–85. [PubMed: 11487631]

Bourinet E, Alloui A, Monteil A, Barrère C, Couette B, Poirot O, Pages A, Mcrory J, Snutch TP, Eschalier A, Nargeot J. Silencing of the Cav3.2 T-type calcium channel gene in sensory neurons demonstrates its major role in nociception. EMBO J. 2005; 24:315–324. [PubMed: 15616581]

Carbone E, Lux HD. A low voltage-activated, fully inactivating Ca^{2+} channel in vertebrate sensory neurones. Nature. 1984; 310:501–502. [PubMed: 6087159]

Cardenas CG, Del Mar LP, Scroggs RS. Variation in serotonergic inhibition of calcium channel currents in four types of rat sensory neurons differentiated by membrane properties. J Neurophysiol. 1995; 74:1870–1879. [PubMed: 8592180]

Choe W, Messinger RB, Leach E, Eckle VS, Obradovic A, Salajegheh R, Jevtovic-Todorovic V, Todorovic SM. TTA-P2 is a potent and selective blocker of T-type calcium channels in rat sensory neurons and a novel antinociceptive agent. Mol Pharmacol. 2011; 80:900–910. [PubMed: 21821734]

Choi S, Na HS, Kim J, Lee J, Lee S, Kim D, Park J, Chen CC, Campbell KP, Shin HS. Attenuated pain responses in mice lacking $Ca_V3.2$ T-type calcium channels. Genes Brain Behav. 2007; 6:425–431. [PubMed: 16939637]

Coste B, Crest M, Delmas P. Pharmacological dissection and distribution of NaN/$Na_V1.9$, T-type Ca^{2+} currents and mechanically activated cation currents in different populations of DRG neurons. J Gen Physiol. 2007; 129:57–77. [PubMed: 17190903]

Dogrul A, Gardell LR, Ossipov MH, Tulunay FC, Lai J, Porecca F. Reversal of experimental neuropathic pain by T-type calcium channel blockers. Pain. 2003; 105:159–168. [PubMed: 14499432]

Dubreuil A, Boukhaddaoui H, Desmadryl G, Martinez-Salgado C, Moshourab R, Lewin GR, Caroll P, Valmier J, Scamps F. Role of T-type calcium current in identified d-hair mechanoreceptor neurons studied in vitro. J Neurosci. 2004; 24:8480–8484. [PubMed: 15456821]

Goldstein ME, House SB, Gainer H. NF-L and peripherin immunoreactivities define distinct classes of rat sensory ganglion cells. J Neurosci Res. 1991; 30 (1):92–104. [PubMed: 1795410]

Guo A, Vulchanova L, Wang J, Li X, Elde R. Immunocytochemical localization of the vanilloid receptor 1 (VR1): relationship to neuropeptides, the P2X3 purinoceptor and IB4 binding sites. Eur J Neurosci. 1999; 11(3):946–58. [PubMed: 10103088]

Lawson SN. The postnatal development of large light and small dark neurons in mouse dorsal root ganglia: a statistical analysis of cell membrane and size. J Neurocytol. 1979; 8:22395–400.

Harper AA, Lawson SN. Conduction velocity is related to morphological cell type in rat dorsal root ganglion neurons. J Physiol Lond. 1985; 359:31–46. [PubMed: 3999040]

Hunt SP, Mantyh PW. The molecular dynamics of pain control. Nat Rev Neurosci. 2001; 2:83–91. [PubMed: 11252998]

Jacus MO, Uebele VN, Renger JJ, Todorovic SM. Presynaptic $Ca_V3.2$ channels regulate excitatory neurotransmission in nociceptive dorsal horn neurons. J Neurosci. 2012; 32(27):9374–82. [PubMed: 22764245]

Jagodic MM, Pathirathna S, Joksovic PM, Lee WY, Nelson MT, Su P, Naik AK, Jevtovic-Todorovic V, Todorovic SM. Up-regulation of the T-type Ca^{2+} current in small rat sensory neurons after chronic constrictive injury of the sciatic nerve. J Neurophysiol. 2008; 99:3151–3156. [PubMed: 18417624]

Jagodic MM, Pathirathna S, Nelson MT, Mancuso S, Joksovic PM, Rosenberg ER, Bayliss DA, Jevtovic-Todorovic V, Todorovic SM. Cell-specific alterations of T-type calcium current in painful diabetic neuropathy enhance excitability of sensory neurons. J Neurosci. 2007; 27:3305–3316. [PubMed: 17376991]

Latham JR, Pathirathna S, Jagodic MM, Choe WJ, Levin ME, Nelson MT, Lee WY, Krishnan K, Covey D, Todorovic SM, Jevtovic-Todorovic V. Selective T-type calcium channel blockade alleviates hyperalgesia in ob/ob mice. Diabetes. 2009; 58(11):2656–65. [PubMed: 19651818]

Lee WY, Orestes P, Latham J, Naik AK, Nelson MT, Vitko I, Perez-Reyes E, Jevtovic-Todorovic V, Todorovic SM. Molecular mechanisms of lipoic acid modulation of T-type calcium channels in pain pathway. J Neurosci. 2009; 29(30):9500–9. [PubMed: 19641113]

Liu Q, Tang Z, Surdenikova L, Kim S, Patel KN, Kim A, Ru F, Guan Y, Weng HJ, Geng Y, Undem BJ, Kollarik M, Chen ZF, Anderson DJ, Dong X. Sensory neuron-specific GPCR Mrgprs are itch

receptors mediating chloroquine-induced pruritus. Cell. 2009; 139(7):1353–65. [PubMed: 20004959]

Matsubara A, Laake JH, Davanger S, Usami S, Ottersen OP. Organization of AMPA receptor subunits at a glutamate synapse: a quantitative immunogold analysis of hair cell synapses in the rat organ of Corti. J Neurosci. 1996; 16(14):4457–67. [PubMed: 8699256]

Marger F, Gelot A, Alloui A, Matricon J, Ferrer JF, Barrère C, Pizzoccaro A, Muller E, Nargeot J, Snutch TP, Eschalier A, Bourinet E, Ardid D. T-type calcium channels contribute to colonic hypersensitivity in a rat model of irritable bowel syndrome. Proc Natl Acad Sci U S A. 2011; 5:108(27):11268–73. [PubMed: 21690417]

McKay BE, McRory JE, Molineux ML, Hamid J, Snutch TP, Zamponi GW, Turner RW. Ca(V)3 T-type calcium channel isoforms differentially distribute to somatic and dendritic compartments in rat central neurons. Eur J Neurosci. 2006; 24(9):2581–94. [PubMed: 17100846]

Messinger RB, Naik AK, Jagodic MM, Nelson MT, Lee WY, Choe WJ, Orestes P, Latham JR, Todorovic SM, Jevtovic-Todorovic V. In vivo silencing of the $Ca_V3.2$ T-type calcium channels in sensory neurons alleviates hyperalgesia in rats with streptozocin-induced diabetic neuropathy. Pain. 2009; 145:184–195. [PubMed: 19577366]

Nelson MT, Joksovic PM, Perez-Reyes E, Todorovic SM. The endogenous redox agent L-cysteine induces T-type Ca^{2+} channel-dependent sensitization of a novel subpopulation of rat peripheral nociceptors. J Neurosci. 2005; 25:8766–8775. [PubMed: 16177046]

Nelson MT, Woo J, Kang HW, Vitko I, Barrett PQ, Perez-Reyes E, Lee JH, Shin HS, Todorovic SM. Reducing agents sensitize C-type nociceptors by relieving high-affinity zinc inhibition of T-type calcium channels. J Neurosci. 2007; 27(31):8250–60. [PubMed: 17670971]

Orestes P, Bojadzic D, Lee J, Leach E, Salajegheh R, Digruccio MR, Nelson MT, Todorovic SM. Free radical signaling underlies inhibition of $Ca_V3.2$ T-type calcium channels by nitrous oxide in the pain pathway. J Physiol. 2011; 589.1:135–148. [PubMed: 21059758]

Perez-Reyes E. Molecular physiology of low-voltage-activated T-type calcium channels. Physiol Rev. 2003; 83:117–161. [PubMed: 12506128]

Rasband MN, Park EW, Vanderah TW, Lai J, Porreca F, Trimmer JS. Distinct potassium channels on pain-sensing neurons. Proc Natl Acad Sci U S A. 2001; 98(23):13373–8. [PubMed: 11698689]

Schroeder JE, Fischbach PS, McCleskey EW. T-type calcium channels: heterogeneous expression in rat sensory neurons and selective modulation by phorbol esters. J Neurosci. 1990; 10(3):947–951. [PubMed: 2156966]

Scroggs RS, Fox AP. Calcium current variation between acutely isolated rat dorsal root ganglion neurons of different size. J Physiol. 1992; 445:639–658. [PubMed: 1323671]

Shin JB, Martinez-Salgado C, Heppenstall PA, Lewin GR. A T-type calcium channel required for normal function of a mammalian mechanoreceptor. Nat Neurosci. 2003; 6(7):724–30. [PubMed: 12808460]

Snider WD, McMahon SB. Tackling pain at the source: new ideas about nociceptors. Neuron. 1998; 20:629–632. [PubMed: 9581756]

Spitzer MJ, Reeh PW, Sauer SK. Mechanisms of potassium- capsaicin-induced axonal calcitonin gene-related peptide release: involvement of L- and T-type calcium channels and TRPV1 but not sodium channels. Neuroscience. 2008; 151(3):836–42. [PubMed: 18178321]

Stucky CL, Lewin GR. Isolectin B4-positive and -negative nociceptors are functionally distinct. J Neurosci. 1999; 19:6497–6505. [PubMed: 10414978]

Sun C, Mtchedlishvili Z, Erisir A, Kapur J. Diminished neurosteroid sensitivity of synaptic inhibition and altered location of the α4 subunit of $GABA_A$ receptors in an animal model of epilepsy. J Neurosci. 2007; 27(46):12641–12650. [PubMed: 18003843]

Takahashi T, Aoki Y, Okubo K, Maeda Y, Sekiguchi F, Mitani K, Nishikawa H, Kawabata A. Upregulation of Ca(v)3.2 T-type calcium channels targeted by endogenous hydrogen sulfide contributes to maintenance of neuropathic pain. Pain. 2010; 150(1):183–91. [PubMed: 20546998]

Talley EM, Cribbs LL, Lee JH, Daud A, Perez-Reyes E, Bayliss DA. Differential distribution of three members of a gene family encoding low voltage-activated (T-type) calcium channels. J Neurosci. 1999; 19:1895–1911. [PubMed: 10066243]

Todorovic SM, Jevtovic-Todorovic V. T-type voltage-gated calcium channels as targets for the development of novel pain therapies. British J Pharmacol. 2011; 163:484–495.

Todorovic SM, Jevtovic-Todorovic V, Meyenburg A, Mennerick S, Perez-Reyes E, Romano C, Olney JW, Zorumski CF. Redox modulation of T-type calcium channels in rat peripheral nociceptors. Neuron. 2001; 31:75–85. [PubMed: 11498052]

Todorovic SM, Lingle CJ. Pharmacological properties of T-type Ca^{2+} current in adult rat sensory neurons: effects of anticonvulsant and anesthetic agents. J Neurophysiol. 1998; 79:240–252. [PubMed: 9425195]

Todorovic SM, Pathirathna S, Brimelow BC, Jagodic MM, Ko SH, Jiang X, Nilsson KR, Zorumski CF, Covey DF, Jevtovic-Todorovic V. 5β-reduced neuroactive steroids are novel voltage-dependent blockers of T-type Ca2+ channels in rat sensory neurons in vitro and potent peripheral analgesics in vivo. Mol Pharmacol. 2004; 66:1223–1235. [PubMed: 15280444]

Zylka MJ, Rice FL, Anderson DJ. Topographically distinct epidermal nociceptive circuits revealed by axonal tracers targeted to Mrgprd. Neuron. 2005; 45:17–25. [PubMed: 15629699]

1. We studied $Ca_V3.2$ expression in peripheral sensory neurons
2. Anti $Ca_V3.2$ antibody labeled mostly small size dissociated sensory neurons
3. Anti $Ca_V3.2$ antibody labeled mostly un-myelinated fibers in sciatic nerve
4. Anti $Ca_V3.2$ antibody labeled nociceptive nerve endings in the skin
5. The study of peripheral $Ca_V3.2$ expression supports its major role in nociception

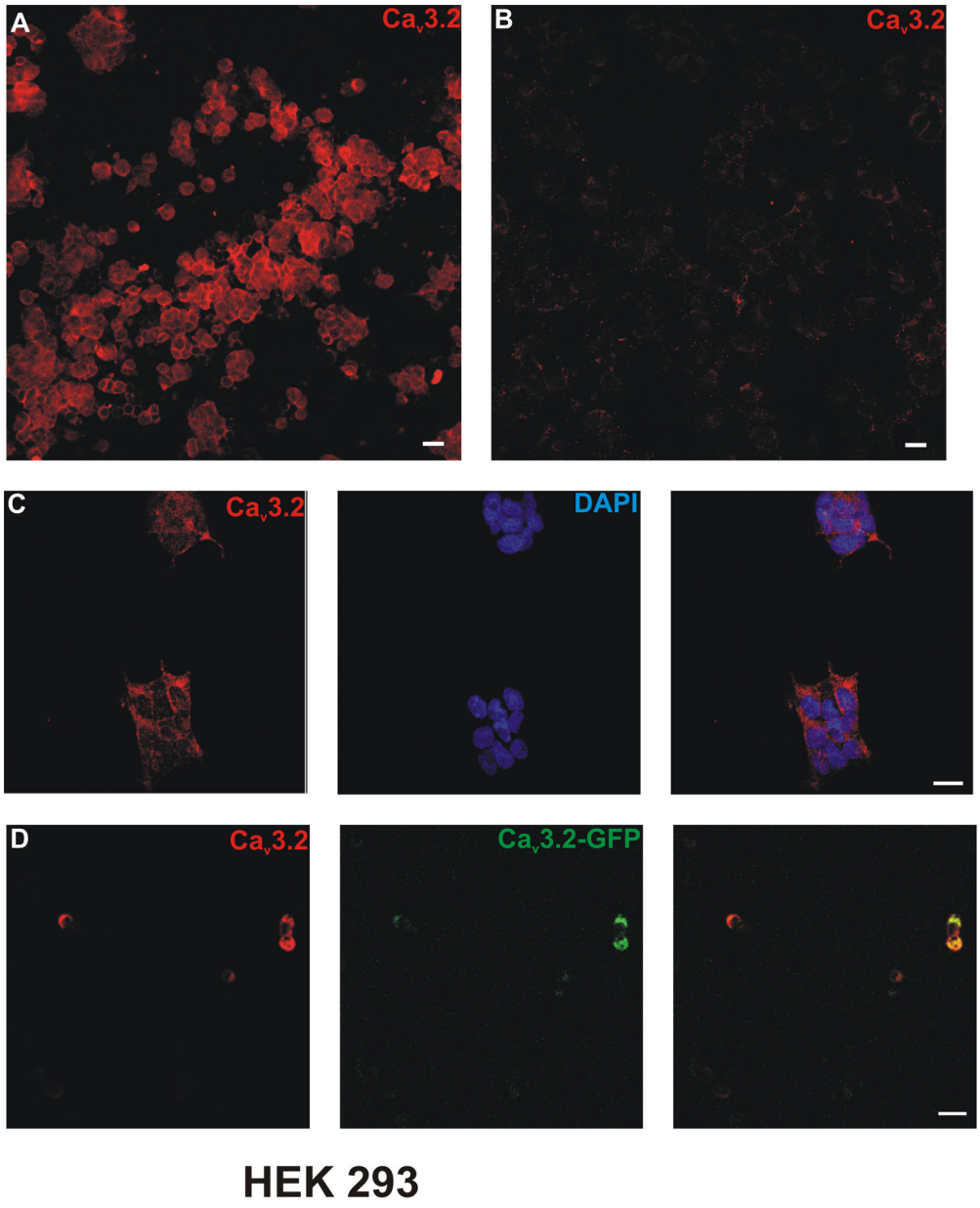

Figure 1. $Ca_v3.2$ antibody labelled protein expression in stable $Ca_v3.2$ expressing HEK-293 cells

Confocal microscopy revealed that $Ca_v3.2$ immunostaining was present within a HEK-293 cell line with stable $Ca_v3.2$ channel expression. A, C) $Ca_v3.2$ immunostaining was seen within HEK-293 cells which stably express $Ca_v3.2$ channel. B) There was no $Ca_v3.2$ labelling within non-transfected wild-type HEK-293 cells. D) $Ca_v3.2$ immunolabeling was also seen within HEK-293 cells transiently transfected with GFP-tagged $Ca_v3.2$ channel. Scale bars = 20μm.

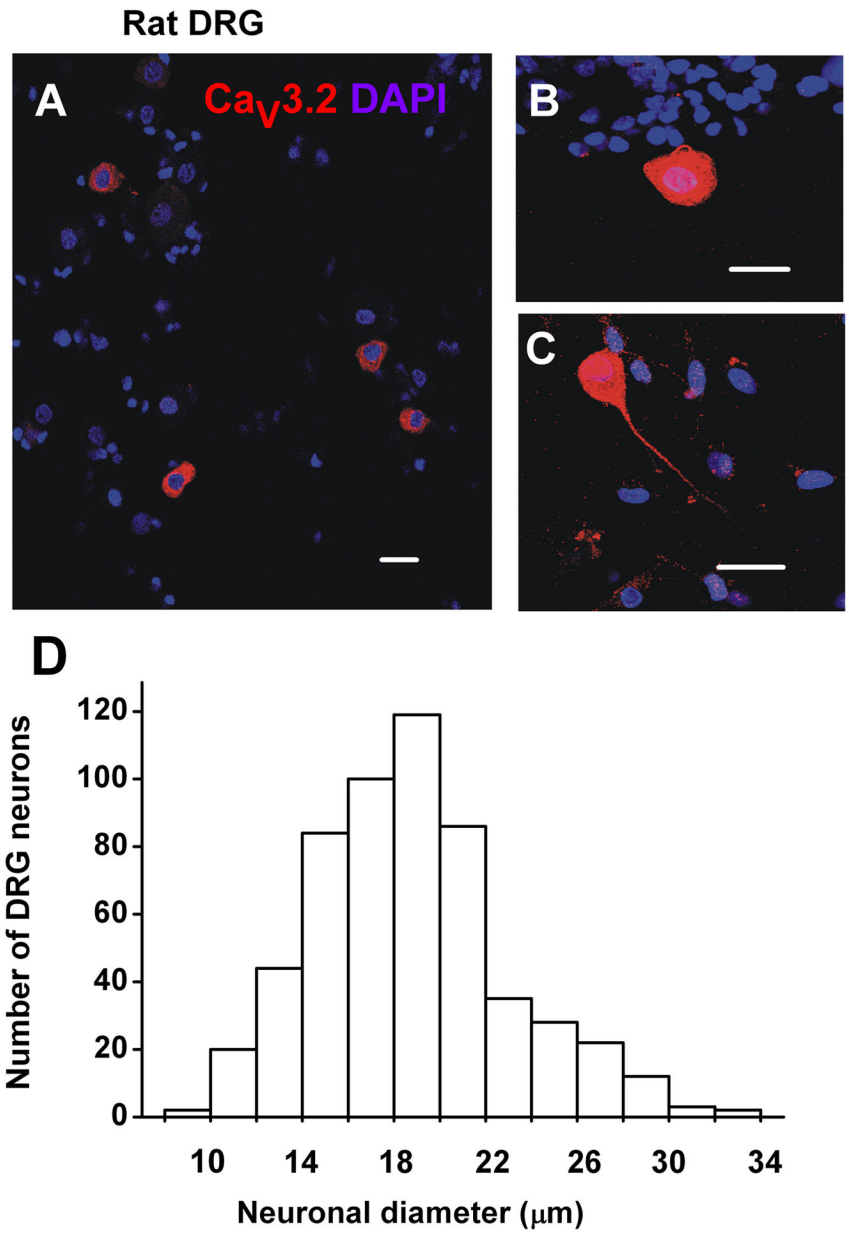

Figure 2. $Ca_v3.2$ immunostaining was predominantly expressed within smaller neurons from acutely dissociated DRG cultures from rat

Confocal microscopy revealed that $Ca_v3.2$ immunolabelling was seen in smaller neurons within heterologous cell cultures from acutely dissociated rat DRG. A) Dissociated DRG cultures contain neuronal and glial cells. Within these cultures, $Ca_v3.2$ immunolabelling was seen within neuronal cells. B–C) $Ca_v3.2$ immunostaining was seen throughout the cell soma and also within somatic sprouts (B) and axons (C) of smaller DRG neurons grown in short – term cultures. D) The graph shows distribution frequency of acutely dissociated DRG cells with different diameters. The median cell diameter of $Ca_v3.2$ immunolabelled neurons was 19 ± 0.2 μm, suggesting that the majority of labelled cells were small sensory neurons. Scale bars = 20 μm.

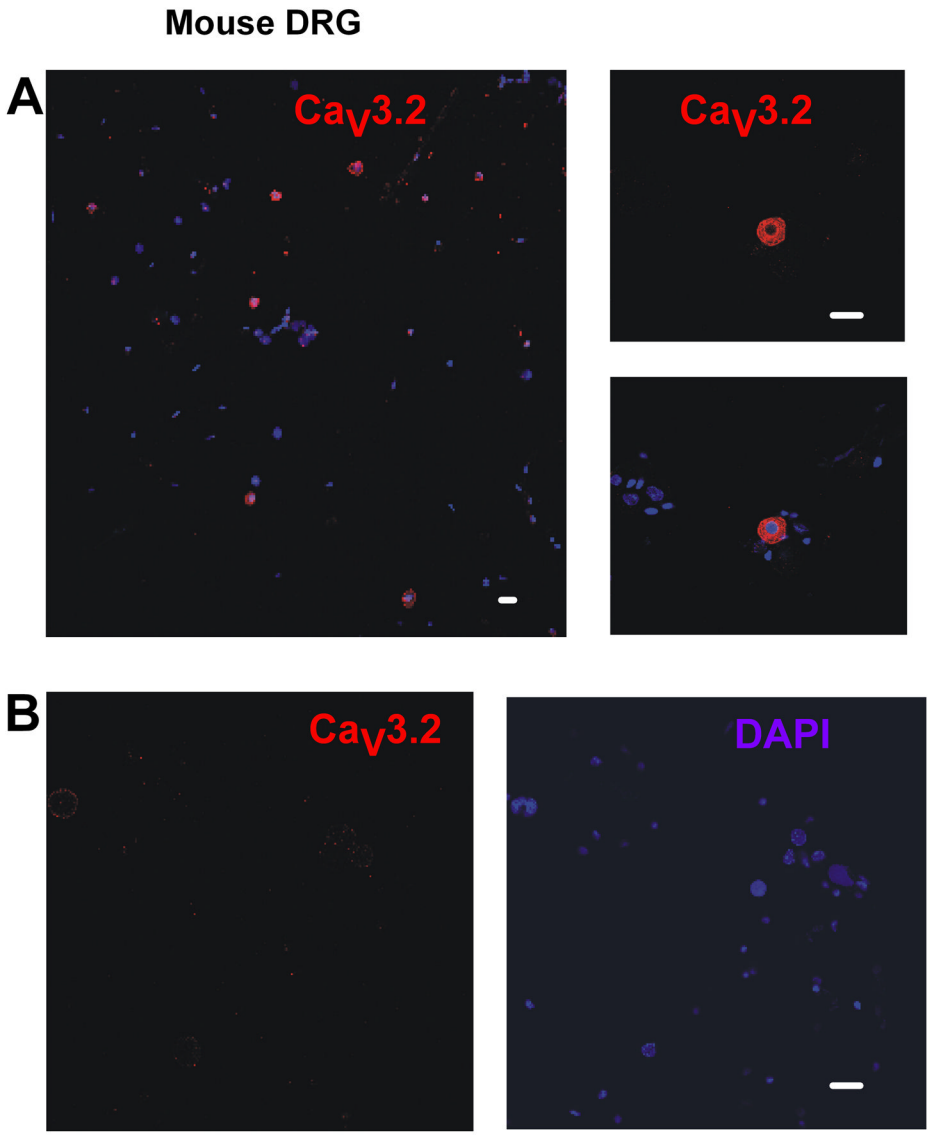

Figure 3. $Ca_V3.2$ immunostaining was present within the sensory neurons of WT mice DRG cultures but was absent from those of $Ca_V3.2$-KO mouse

Confocal microscopy revealed that $Ca_V3.2$ immunostaining was seen within smaller DRG neurons of WT mouse in short-term DRG cultures but not within DRG cultures from $Ca_V3.2$ KO mice. A) $Ca_V3.2$ immunolabeling was present within a proportion of DRG sensory neurons from WT mice cultures. B) $Ca_V3.2$-KO mouse DRG cultures showed no $Ca_V3.2$-positive immunolabeling. Scale bars = 20 μm.

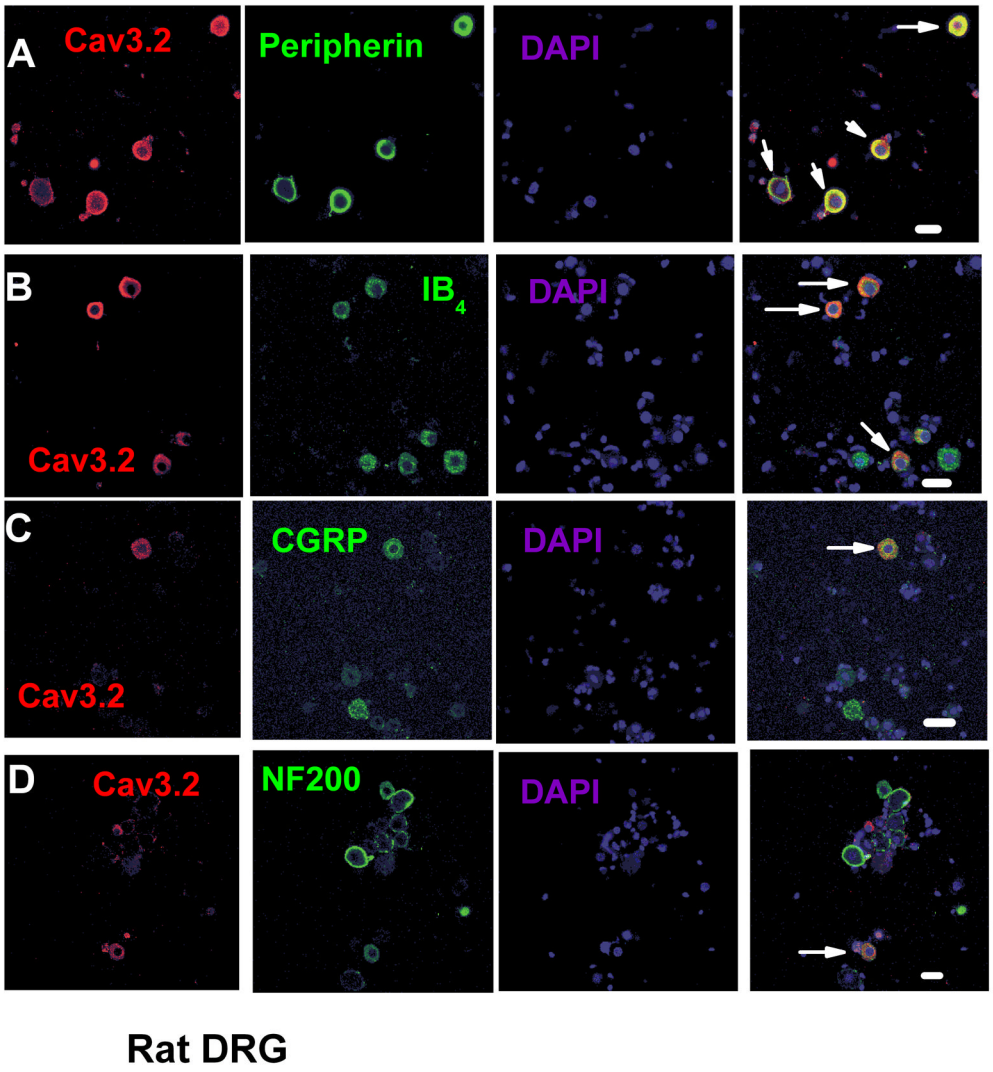

Figure 4. $Ca_V3.2$ immunolabelling was colocalised with distinct neuronal markers within dissociated DRG cultures

Confocal microscopy revealed that $Ca_V3.2$- expressing DRG neurons also expressed nociceptive markers. A) Most of $Ca_V3.2$-positive cells also expressed peripherin, a marker of nonmyelinated sensory neurons. B) $Ca_V3.2$-positive neurons also co-expressed IB_4, a marker of nonpeptidergic nociceptive sensory neurons. C) Some $Ca_V3.2$-labelled neurons were also positive for CGRP, a marker of peptidergic sensory neurons. D) Fewer $Ca_V3.2$ labelled neurons were also found expressed with NF200, a marker of myelinated sensory neurons. Scale bars = 20 μm.

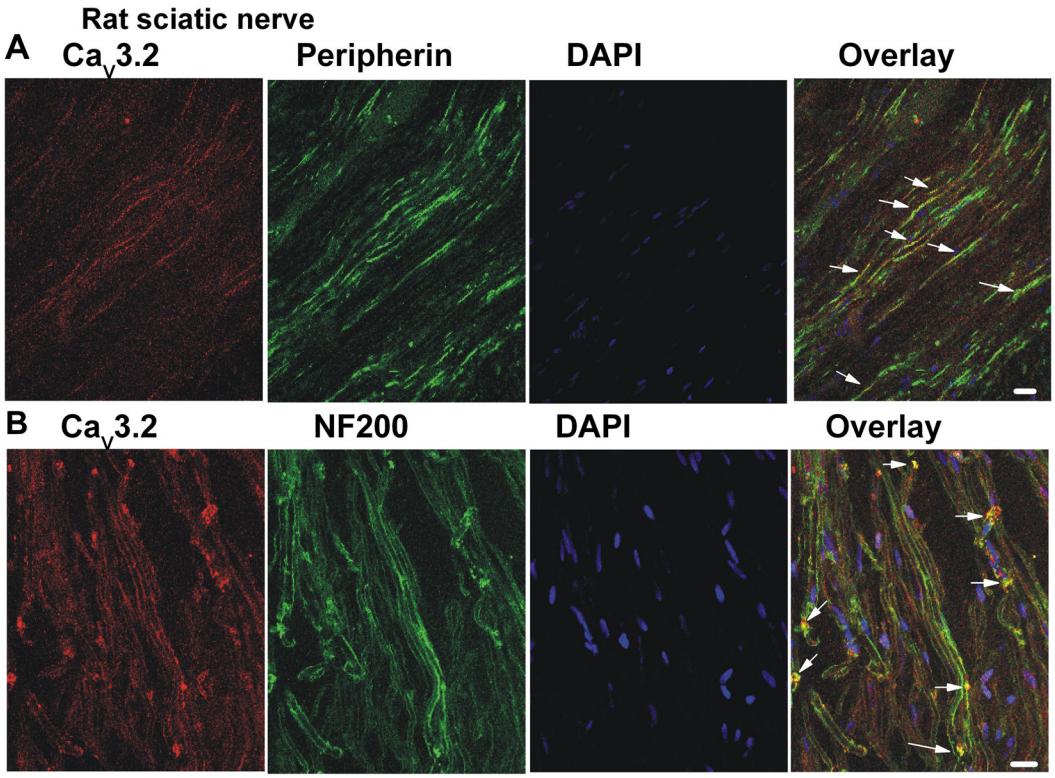

Figure 5. $Ca_V3.2$ immunostaining was found within rat sciatic nerve co-expressed with nerve fibre markers

Confocal microscopy revealed that $Ca_V3.2$ expression was found within rat sciatic nerve. $Ca_V3.2$ positive fibres were often colocalised with peripherin (panel A) and NF200 (panel B). Panels from the left to the right show staining with anti-$Ca_V3.2$ antibody (red), peripherin (green, A) or NF200 (green, B), DAPI (blue) and overlay as indicated by yellow colour and arrows. Scale bars = 20 μm.

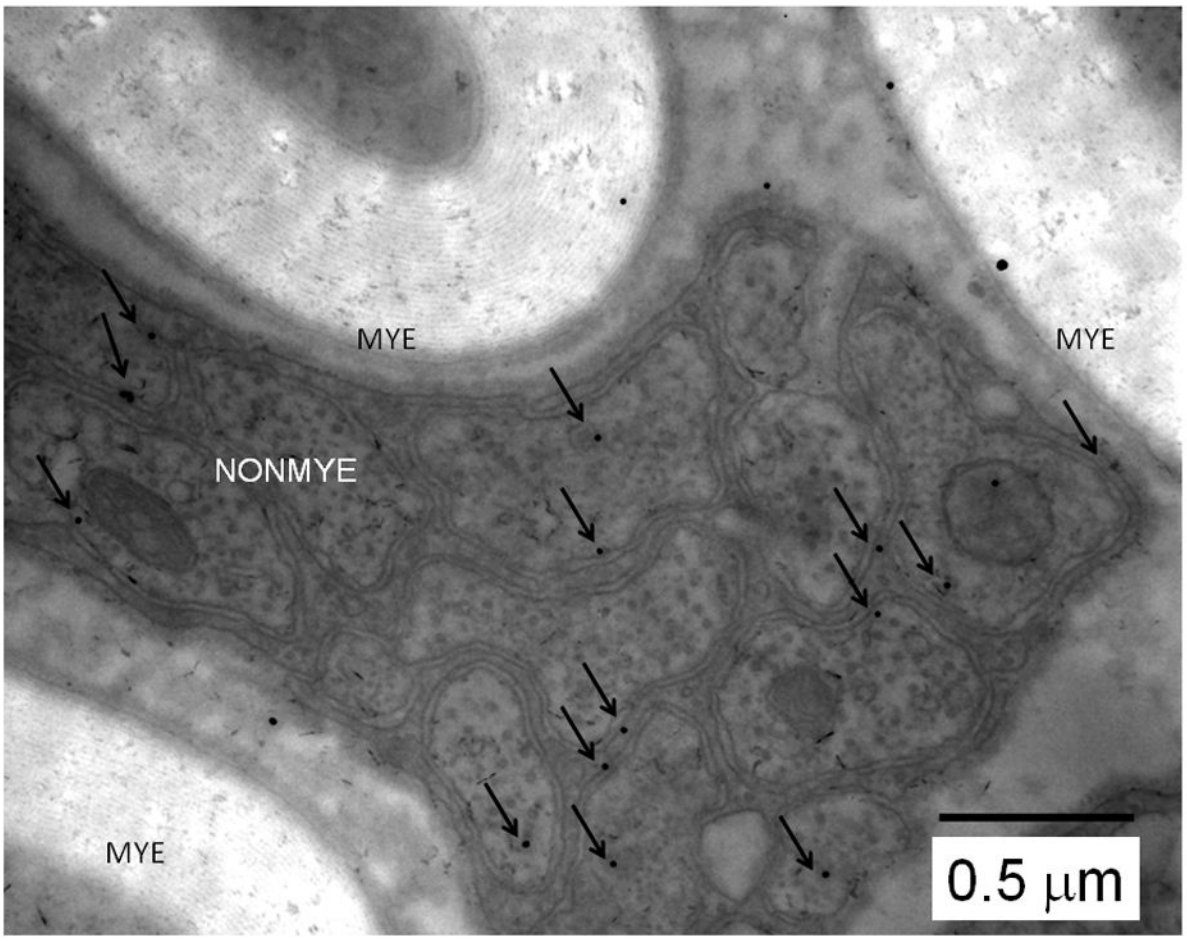

Figure 6. $Ca_V3.2$ immunostaining was found in nonmylelinated fibres of the mouse sciatic nerve

High-magnification micrograph where dots represent gold-conjugated anti-$Ca_V3.2$ antibody staining of sciatic nerve fibres of WT mouse. Note that $Ca_V3.2$-positive immunoreactivity is largely associated with the membranes of nonmyelinated (NONMYE) nerve fibres and is much less prominent on myelinated (MYE) fibres as indicated by arrows. Arrows show gold particles that within 100 nm of axonal membrane. Scale bar = 500 nm.

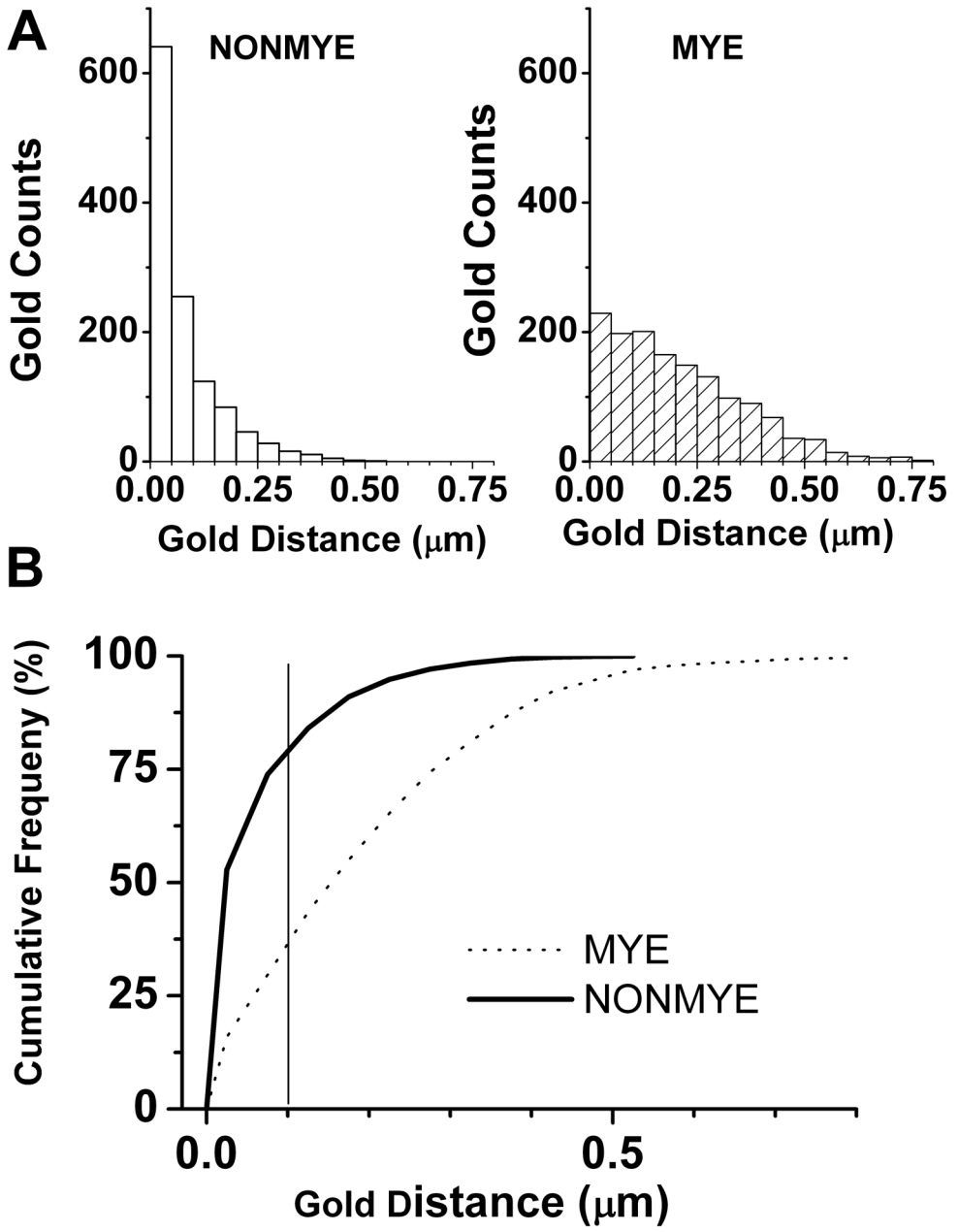

Figure 7. Quantification of $Ca_V3.2$ expression in sciatic nerve of mouse using EM

A) The graphs show distribution of the gold-conjugated $Ca_V3.2$ immunoparticles as determined by their distance from axonal membranes in NONMYE (open bars on the left) and MYE (cross-hatched bars on the right).

B) The graph shows cumulative frequency of the distributions of Cav3.2 immunoparticles as determined in experiments depicted on the panels A of this figure. Note that black solid line (NONMYE) is largely shifted to the left when compared to dotted line (MYE) indicating closer association of $Ca_V3.2$ with axonal membranes of NONMYE. Solid vertical gray line represents the distance of 0.1 μm from the membrane. For the experiments depicted on this figure we analyzed 41 EM microphotographs and performed a total of 2514 measurements.

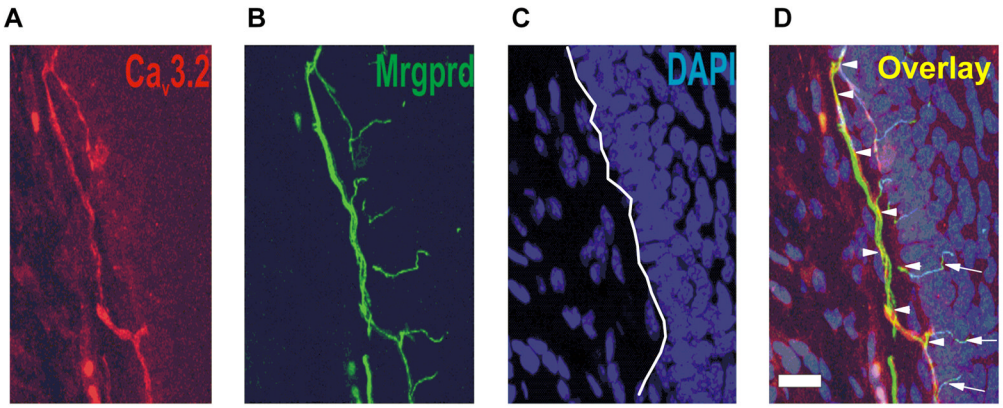

Figure 8. $Ca_V3.2$ immunostaining was found within the dermal-epidermal layer of glaborous skin from the mouse hind paw

Confocal microscopy revealed that expression of $Ca_V3.2$-positive fibre (red) was found within the dermal-epidermal border of Mrgprd-KI mouse hind paw (E). Panel F shows Mrgprd positive fibres (green) in the same slide as panel A. Panel C of this figure shows outlines of cell's nuclei on same slide stained with DAPI (blue). Panel H shows overlay of staining (yellow) depicted on panels E, F and G. Note that $Ca_V3.2$ immunostaining was largely co-localized with Mrgprd staining. Scale bars = 20 μm.

Table 1

Primary and secondary antibody information.

Primary Antibody	DRG	Nerve	Skin	Supplier	Secondary Antibody	Supplier
Rabbit anti-Cav3.2	1:500	1:250	1:100	Sigma	Donkey anti-Rabbit Alexa555	Invitrogen
FITC-conjugated anti-IB4	1:500	-	-	Sigma	-	-
Mouse anti-NF200	1:500	1:100	1:100	Sigma	Donkey anti-Mouse Alexa488	Invitrogen
Chicken anti-peripherin	1:250	1:100	1:100	Aves Lab	Donkey anti-Chicken DyLight488	Jackson Immuno Research
Mouse anti-CGRP	1:500	-	-	Sigma	Donkey anti-Mouse Alexa488	Invitrogen